Computational analysis of the quaternary structural changes induced by point mutations in human UDP-glucose dehydrogenase

ARTICLE *in* ARCHIVES OF BIOCHEMISTRY AND BIOPHYSICS · MAY 2009

Impact Factor: 3.02 · DOI: 10.1016/j.abb.2009.03.017 · Source: PubMed

7 AUTHORS, INCLUDING:

Chae Hun Leem
University of Ulsan
39 PUBLICATIONS **320** CITATIONS

SEE PROFILE

Han Choe
Asan Medical Center
83 PUBLICATIONS **1,290** CITATIONS

SEE PROFILE

Archives of Biochemistry and Biophysics 486 (2009) 35–43

Contents lists available at ScienceDirect

Archives of Biochemistry and Biophysics

journal homepage: www.elsevier.com/locate/yabbi

Computational analysis of the quaternary structural changes induced by point mutations in human UDP-glucose dehydrogenase

Hui Sun Lee, Young Jin Son, Seon Ha Chong, Ji Young Bae, Chae Hun Leem, Yeon Jin Jang, Han Choe *

Department of Physiology and Research Institute for Biomacromolecules, University of Ulsan College of Medicine. Seoul 138-736, South Korea

ARTICLE INFO

Article history:
Received 9 February 2009
and in revised form 12 March 2009
Available online 7 April 2009

Keywords:
UDP-glucose dehydrogenase
Oligomeric state
Hexamer
Dimer
Normal mode analysis
Motional fluctuation
Oligomeric interface

ABSTRACT

UDP-glucose dehydrogenase (UGDH) is an enzyme catalyzing the conversion of UDP-glucose to UDP-glucuronic acid. Site-directed mutagenesis studies have revealed that human UGDH (hUGDH) has distinct oligomeric states that vary with different point mutations. In this study we have investigated how the changes in the oligomer-forming propensity may be involved in the thermal motion of wild-type hUGDH and its mutants, using normal mode analysis (NMA). Our results show that the perturbation caused by the mutation of a residue at a considerably distant location from the oligomeric interfaces is preferentially distributed throughout specific sites, especially the large flexible regions in the hUGDH structure, thereby changing the motional fluctuation pattern at the oligomeric interfaces. A large-magnitude cooperative motion at the oligomeric interfaces is a critical factor in interfering with the hexamer formation of the enzyme. In particular, structural stability at the dimeric interface is necessary to retain the hexameric structure of hUGDH.

Introduction

UDP-glucose dehydrogenase (UGDH)[1] catalyzes the conversion of UDP-glucose to UDP-glucuronic acid through two successive nicotinamide adenine dinucleotide (NAD^+)-dependent oxidation steps [1]. In mammals, UDP-glucuronic acid is the substrate for UDP-glucuronosyltransferase that transfers glucuronic acid to available substances, such as steroids, bile acids, bilirubin, hormones, dietary constituents, and xenobiotics, to generate glucuronides in the liver [2,3]. UDP-glucuronic acid is also an essential precursor for synthesis of various glycosaminoglycans (GAGs) such as hyaluronan (HA), heparin sulfate, and chondroitin sulfate [4]. GAGs are ubiquitous components of extracellular matrices and pericellular spaces that perform critical roles in various aspects of cell behavior, including signal transduction, cell proliferation, cell spreading, cell migration, and cancer development [5–8]. Because UDP-glucuronic acid is necessary for GAG synthesis, any regulation of UGDH activity may influence proteoglycan structure and function [9]. Increased levels of HA in tumor cells indicate that the inhibition of UGDH may restrict tumor growth, implying that UGDH could be a novel cancer therapeutic target [10,11]. Therefore, an understanding of the structural characteristics of the enzyme at a molecular level would be useful in developing rational strategies for ligand design.

The first published UGDH structure was that of the *Streptococcus pyogenes* (*S. pyogenes*) enzyme, determined by X-ray crystallography [12]. This structure demonstrated a crystallographic homodimer, with the monomer composed of two discrete α/β domains, each of which contained a core β-sheet sandwiched between α-helices. These two α/β domains were connected by a long central α-helix providing a major dimeric interface. The six-stranded parallel β-sheet, which is characteristic of the dinucleotide-binding Rossmann fold, serves as the core of NAD^+-binding at the N-terminal α/β domain. The C-terminal α/β domain has a five-stranded parallel β-sheet with α-helices packed on either side, and contains the UDP moiety of the UDP-sugar in a deep pocket.

Human UGDH (hUGDH) has 23% sequence identity with the *S. pyogenes* enzyme [13]. Recently, the X-ray crystal structure of hUGDH has been deposited in the Protein Data Bank (PDB ID: 2q3e) [14]. Each subunit and dimer show great architectural and structural homology to those of *S. pyogenes* (Fig. 1a and b). However, the oligomeric state of hUGDH is a crystallographic hexamer, composed a "trimer of dimers" [1] (Fig. 1c and d).

Flexibility and internal motions of proteins are essential for their biological functions [15,16]. Computational approaches are powerful methods that enable us to explore the thermally driven

* Corresponding author. Fax: +82 2 3010 8029.
E-mail addresses: hchoe@amc.seoul.kr (H. Choe).

[1] *Abbreviation used:* UGDH, UDP-glucose dehydrogenase; NMA, normal mode analysis; hUGDH, human UGDH; GAGs, glycosaminoglycans; HA, hyaluronan; NAD^+, nicotinamide adenine dinucleotide; PDB, Protein Data Bank; NMA, normal mode analysis; SD, steepest descent; PRCG, PR-conjugated gradient; LLMOD, low-mode conformational search procedure; MSF, mean-square fluctuation; RMSD, root-mean-square deviation.

0003-9861/$ - see front matter © 2009 Elsevier Inc. All rights reserved.
doi:10.1016/j.abb.2009.03.017

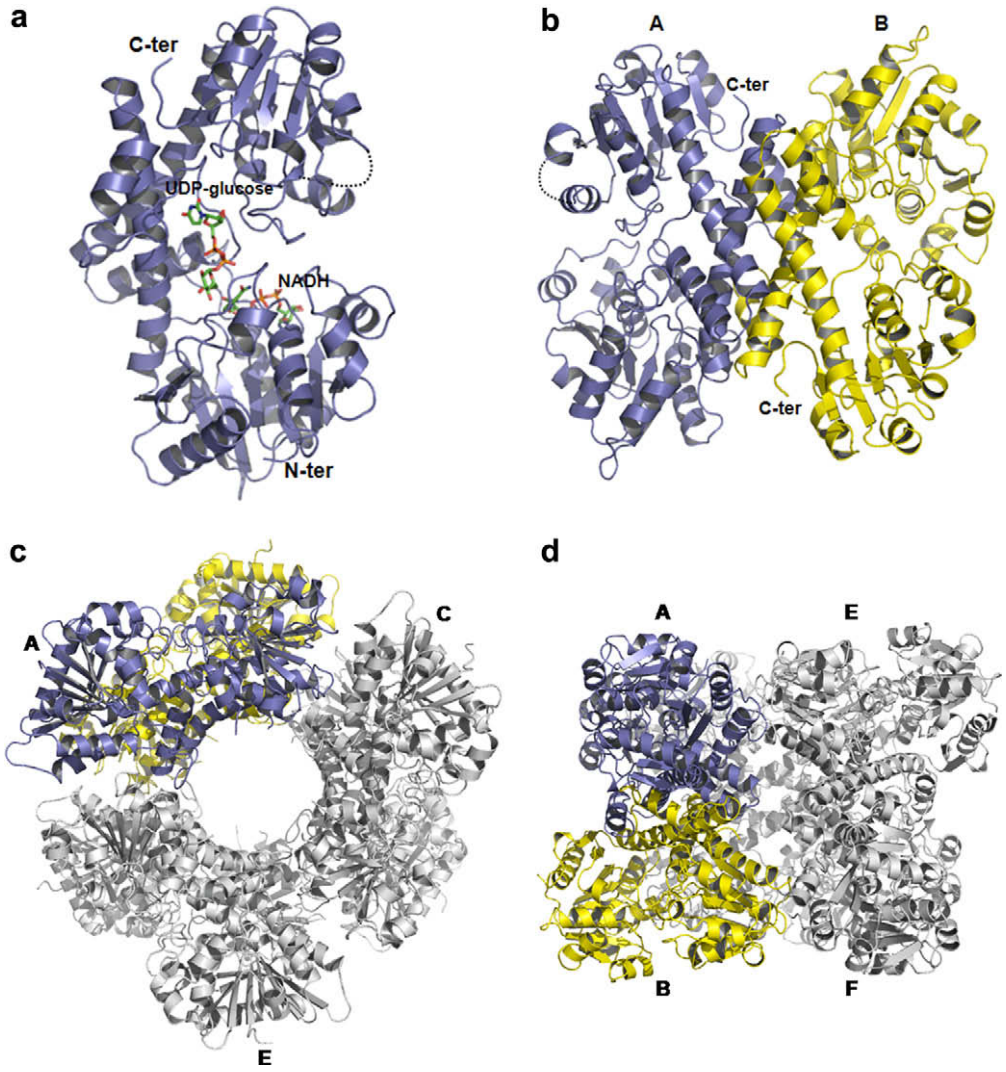

Fig. 1. Structures of hUGDH (PDB ID: 2q3e). The structures are displayed as ribbon representations. The chain identifiers of subunits are also shown on the structures. (a) hUGDH monomer with nicotinamide adenine dinucleotide (NADH) and uridine-5′-diphosphate-glucose (UDP-glucose). (b) hUGDH dimer. NADH and UDP-glucose are removed for clarity. Subunits A and B are colored blue and yellow, respectively. (c) hUGDH hexamer (top view). (d) hUGDH hexamer (side view). All the structural figures were generated using PyMol (DeLano Scientific LLC, San Francisco, CA). (For interpretation of the references to colour in this figure legend, the reader is referred to the web version of this article.)

dynamics of the proteins. Molecular dynamics simulation is a useful technique to investigate details of molecular motions. However, a primary limitation of this method is its inefficiency in sampling large conformational changes on biologically relevant timescales. On the other hand, normal mode analysis (NMA) is a time-independent approach yielding insights into the mechanisms of large-amplitude molecular deformational motions. Despite the limitations of the NMA method due to its simplifying assumptions [17], many studies have revealed that the NMA method is valuable in the description of biologically relevant motions of proteins in terms of coordinates that involve the collective displacement of a large number of atoms [18–20].

In the previous reports of hUGDH single amino acid mutant studies, several residues (K220, C276, K279, D280 and K339) were selected to find out if they are located at the active site so that the mutations alter the catalytic activity [13,21]. The selection was based on the homology model of hUGDH generated from the crystal structure of *S. pyogenes* and previously published biochemical studies of the bacterial enzyme. Multiple sequence alignment shows that the residues at the locations of point mutations are completely conserved between species (Fig. 3). The experimental data revealed the importance of the mutated residues for catalytic activity. A further surprising result was that mutations at these sites altered the oligomeric states of the enzyme, even though the substituted residues do not directly interact with other subunits to form a quaternary structure (Fig. 2c). It remains to be elucidated whether distinct oligomeric states triggered by point mutations have physiological relevance and if subunit association may affect enzyme function.

The main objective of this study is to gain insights into the nature of the alteration in the oligomeric state of hUGDH induced by point mutations. The inherent flexibility of monomeric WT hUGDH and its mutants was analyzed using the NMA method. We test whether these mutations change the dynamics of the protein and therefore have a long-range effect on the oligomeric interfaces. We show that the substitution of residues in the hUGDH structure triggers changes in the motional fluctuation patterns of the protein and that these changes at the oligomeric interfaces are strongly correlated with the oligomer-forming propensity of the enzyme.

a

Region	Sub-region	Residues in chain A	$r_s - r_e$
R_B	R_{B1}	134, 135	134 – 135
	R_{B2}	176,177	176 – 177
	R_{B3}	209, 211, 214, 215, 218, 222, 223, 226, 227, 229, 230, 232, 233, 234, 236, 239, 240, 241, 243, 244, 246, 247, 250, 251, 254, 255, 257, 258, 259, 260, 261, 264, 265, 266	209 – 266
	R_{B4}	284, 287, 288, 291, 293, 295, 296, 298, 299, 300, 302, 306, 309	284 – 309
R_C	R_{C1}	316, 319, 320, 323, 325, 327, 329	316 – 329
	R_{C2}	359, 360	359 – 360
	R_{C3}	409	409
	R_{C4}	434, 435	434 – 435
R_E	R_{E1}	94, 96, 97, 98	94 – 98
	R_{E2}	106, 107, 110, 114	106 –114
	R_{E3}	139, 142, 143, 146, 147	139 – 147
R_F		290, 292	290 – 292

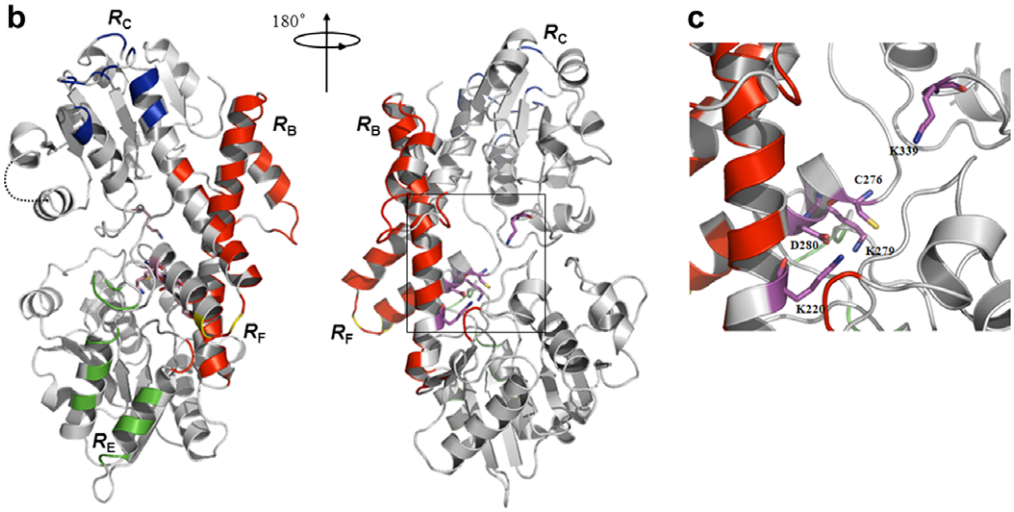

Fig. 2. The residues at oligomeric interfaces and mutated sites. (a) The residues directly interacting with other subunits (closely contacting residues) are shown in the third column of the table. The residues were also grouped into sub-regions in terms of their sequence numbers. In this table, r_s and r_e are the start and end sequence numbers defining each sub-region, respectively. (b) The closely contacting residues are highlighted on the hUGDH structure using different colors: red (R_B); blue (R_C); green (R_E) and yellow (R_F). (c) A magnified image of the boxed region in Fig. 2b. The residues at the mutation sites are illustrated by stick representation. (For interpretation of the references to colour in this figure legend, the reader is referred to the web version of this article.)

```
                180       190       200       210       220       230
Human           IGGDETPEGQRAVQALCAVYEHWVPREKILTTNTWSSELSKLAANAFLAQRISSINSISA
Bovine          IGGDETPEGQRAVQALCAVYEHWVPREKILTTNTWSSELSKLTANAFLAQRISSINSISA
S.pyogenes      VGNESRNSQLFLDILTDISVEKDSP---SLLVGSSEAEAIKLFSNAYLAQKIAFFNEWDT
E.coli          IGECSERAERLAVLFQEGAIKQNIP---VLFTDSTEAEAIKLFSNTYLAMRVAFFNELDS

                240       250       260       270       280       290
Human           LCEATGADVEEVATAIGMDQRIGNKFLKASVGFGGSCFQKDVLNLVYLCEALNLPEVARY
Bovine          LCEATGADVEEVATAIGMDQRIGNKFLKASVGFGGSCFQKDVLNLVYLCEALNLPEVARY
S.pyogenes      FAEMQNLDSKKIIEAMGYDQRIGNSHNNPSFGFGGYCLPKDIKQLEYHFKEIPAPIIT--
E.coli          YAESFGLNTRQIIDGVCLDPRIGNYYNNPSFGYGGYCLPKDTKQLLANYQSVPNKLIS-

                300       310       320       330       340       350
Human           WQQVIDMNDYQRRRFASRIIDSLFNTVTDKKIAILGFAFKKDTGDTRESSSIYISKYLMD
Bovine          WQQVIDMNDYQRRRFASRIIDSLFNTVTDKKIAILGFAFKKDTGDTRESSSIYISKYLMD
S.pyogenes      --SISESNLLRKIHIAKMILN-----SSAKTIGIYRINSKKDSDNCRESSTIDVAKLLKS
E.coli          --AIVDANRTRKDFITNVILK-----HRPQVVGVYRLIMKSGSDNFRDSSILGIIKRIKK
```

Fig. 3. Multiple sequence alignment of four sequences that include human, bovine, *S. pyogenes* and *E. coli* UGDH. The boxed areas correspond to the single mutated sites. Positions of the sites are displayed above the sequence.

Materials and methods

Preparation of initial structures

The starting coordinates were taken from a 2.0 Å X-ray structure of hUGDH (PDB ID: 2q3e). The entire crystallographic structure of the PDB file contains two hexamers (A–F, and G–L as chain identifiers, respectively), in the asymmetric units. Each subunit consisting of the hexamer is complexed with NADH in the N-terminal domain and UDP-glucose in the C-terminal domain. We used the coordinates of subunit A as the starting structure for our modeling studies. The NADH and UDP-glucose were removed from the structure. Six residues (Pro383–Asp388), which are not seen the X-ray crystallographic structure, were modeled and their conformations were refined using MODELLER (version 9.4) [22]. The initial coordinates of all hUGDH mutants were generated by MODELLER using the structure of the subunit A as a template. We refer to these as homology-modeled structures.

Energy minimization of initial structures

The crystallographic WT and its mutants generated by homology modeling were energy-minimized using MacroModel (Schrödinger, LLC, New York, NY). The energy minimization of the structures was performed in the absence of oligomeric constraints. The minimization procedure commenced with 500 steepest descent (SD) steps, followed by application of the PR-conjugated gradient (PRCG) minimization algorithm in the GB/SA implicit solvation model, using the derivative convergence criterion of 10^{-3} kJ/Å-mol. All atomic AMBER* was employed as the force field. vdW and electrostatics were treated using the cutoff distances of 8 Å and 20 Å, respectively. We refer to the structures resulted from the energy minimizations as energy-minimized structures.

Normal mode analysis protocol

Normal modes were calculated using the VBR2 function with ARPACK [23] in the MacroModel suite. VBR2 function utilizes a large-scale low-mode conformational search procedure (LLMOD), which provides a set of eigenvectors and eigenvalues for the vibrational modes of a molecule [24,25]. Normal mode calculations were performed for the energy-minimized structures under the same force field conditions to those used for the energy minimizations. Rotational and translational modes were automatically disregarded. We confirmed that the normal modes calculated for all the energy-minimized structures had no imaginary frequencies.

Calculation of motional fluctuation

The eigenvectors calculated in NMA represent the directions and relative magnitudes of each atomic motion. The corresponding eigenvalues were converted to frequency units for data analysis. The magnitude of atomic displacement in normal mode motions was analyzed based on the mean-square fluctuation (MSF) of the *i*th atomic coordinate. The MSF contribution of the *i*th atom from the *j*th normal mode to the *n*th normal mode is given by [26]:

$$\langle \Delta x_i^2 \rangle = \frac{k_B T}{m_i} \sum_j^n \frac{a_{ij}^2}{\omega_j^2} \quad (1)$$

where m_i is the mass of the *i*th atom, k_B is the Boltzmann constant, and T is the absolute temperature. The term a_{ij} is the normalized mode of atom i under mode j, and ω is the vibrational frequency. Eigenvalues and eigenvectors were obtained for a total of the 106 lowest frequency normal modes and used in calculations of the MSF. The MSF of each residue was represented by that of Cα atom in the corresponding residue.

Motional fluctuation at a region, R, which contains N_R residues from residue sequence number r_s to r_e, was defined as an average MSF over all the residues belonging to the region:

$$\langle \Delta x_R^2 \rangle = \frac{\sum_{i=r_s}^{r_e} \langle \Delta x_i^2 \rangle}{N_R} \quad (2)$$

The motional fluctuation at a large region consisting of several small regions was calculated using similar approach. For example, the motional fluctuation at regions R_1 and R_2 ($R_1 + R_2$) is defined by:

$$\langle \Delta x_{R_1+R_2}^2 \rangle = \frac{\sum_{i=r_{s,R_1}}^{r_{e,R_1}} \langle \Delta x_i^2 \rangle + \sum_{i=r_{s,R_2}}^{r_{e,R_2}} \langle \Delta x_i^2 \rangle}{N_{R_1} + N_{R_2}} \quad (3)$$

where N_{R_1} and N_{R_2} are the numbers of residues in R_1 and R_2, respectively.

Results and discussion

Defining the oligomeric interfaces

The structure of hUGDH in the crystal form reveals a hexameric arrangement, composed a "trimer of dimers" of six subunits (termed subunit A–F in Fig. 1c and d). To determine the oligomeric interfaces in the hUGDH hexamer, we selected the residues of subunit A that were in close contact with other subunits (Fig. 2a and b). When any atom of a residue in subunit A was within 4 Å of any atom of other subunits, the residue was identified as a closely contacting residue. About 78 closely contacting residues were found from a total of 446 residues of subunit A. The regions containing these closely contacting residues were defined as the oligomeric interfaces. Of the 78 residues, 51 were located at a dimeric interface formed by subunit B, and 27 residues were at trimeric interfaces by subunits C, E, and F, indicating that the largest contribution was provided by the dimeric interface. There were no resi-

Table 1
Dimer-forming propensity values of WT hUGDH and its mutants. The values were quantified based on the oligomeric states of the hUGDHs as experimentally observed in the studies by Easley [13], Sommer [21] and Huh [27].

hUGDH	Dimer-forming Propensity
Wild-type and single mutants	
K220A	0
D280N	0
WT	1
C276S	1
C276A	2.5
K279A	5
K339A	5
Double mutant	
A222Q/S233G	5

Table 2
The root-mean-square deviation (RMSD) (Å) from crystal hUGDH structure for the homology-modeled and the energy-minimized structures. The RMSD was computed on the Cα atoms. The correlation coefficient (r) values between the RMSD and dimer-forming propensity are also displayed in the table.

	Homology-model structure	Energy-minimized structure
K220A	0.23	1.22
D280N	0.22	1.12
WT	0	0.97
C276S	0.22	1.29
C276A	0.20	1.06
K279A	0.19	1.48
K339A	0.22	1.12
r	0.13	0.36

dues in close contact with subunit D. We designated the dimeric interface as R_B and the three trimeric interfaces as R_C, R_E and R_F. Residues belonging to each region were further grouped into several sub-regions in terms of their sequence numbers.

Quantifying the oligomer-forming propensities of WT hUGDH and its mutants

Several previous studies have examined the oligomeric states of WT hUGDH and its mutants in solution by gel filtration chromatography. Whereas WT hUGDH was observed to be predominantly a hexamer with a small amount of dimeric forms, the K279A mutant was essentially a dimer. The C276S mutant showed a pattern of peaks similar to that of the WT enzyme [21]. The K220A and D280N mutants showed, exclusively, hexameric quaternary structures in solution. On the other hand, the mutants K339A and C276A were observed to be a dimer and a hexamer-dimer mixture, respectively [13]. Intriguingly, no substituted residues in all the single mutants of hUGDH belonged to the closely contacting residues at the oligomeric interfaces, implying that the residues at

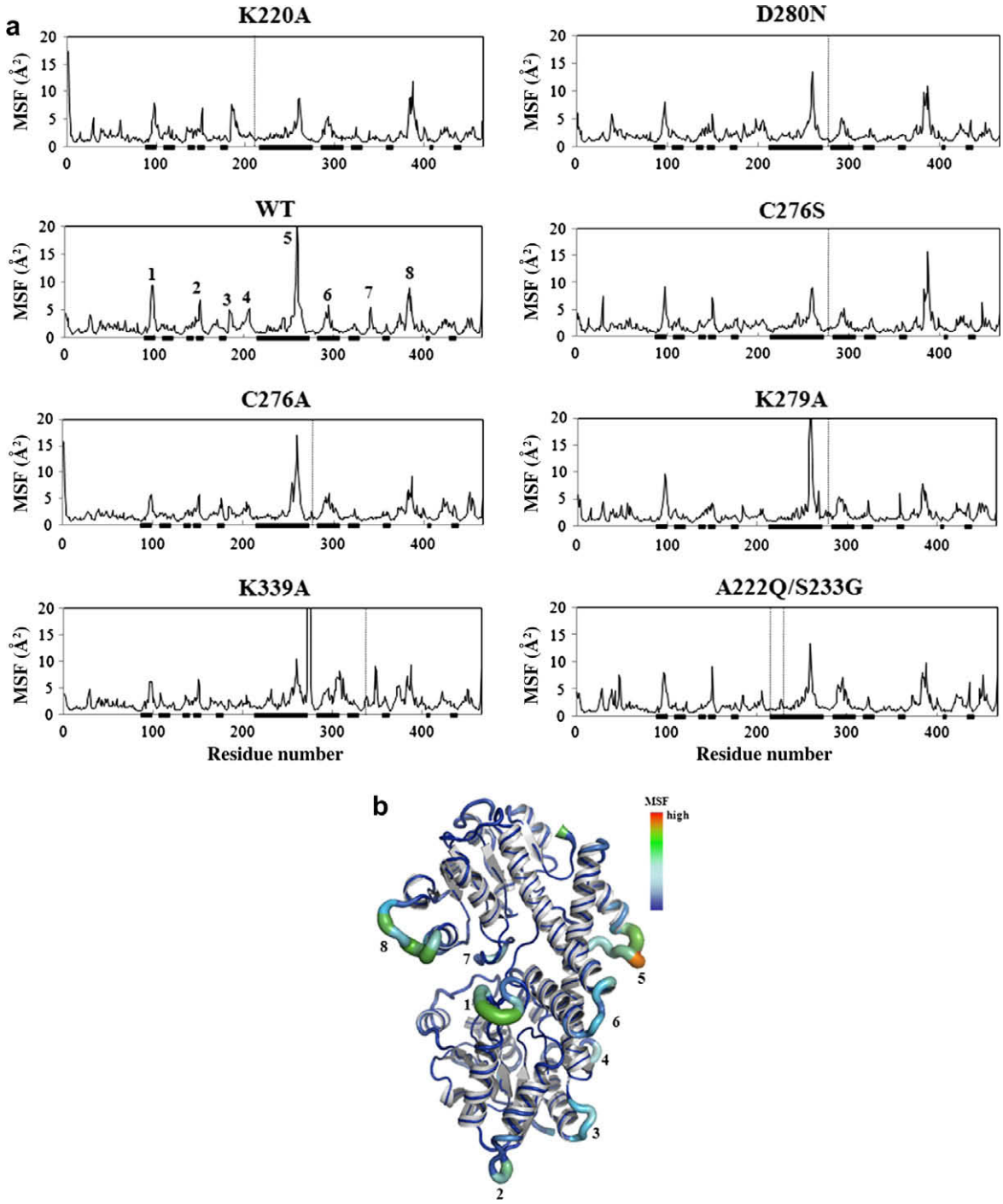

Fig. 4. NMA results for WT hUGDH. (a) Mean-square fluctuation (MSF) plots calculated for WT and all mutant structures. Black thick bars on the horizontal axis of the plot indicate the oligomeric interface regions. Dotted vertical lines in the plots indicate the mutated positions. Eight representative regions of large MSF are also indicated in the plot of WT hUGDH. (b) The MSF of WT hUGDH with respect to the structure is represented by a tube. The tube color and diameter represent the magnitude of the fluctuation. Secondary structures of hUGDH are shown in a ribbon diagram.

the mutated positions do not directly participate in inter-subunit interactions for oligomer formation (Fig. 2). A double mutant hUGDH, A222Q/S233G was a dimer in solution [27]. The mutated A222 and S233, in contrast, were residues directly interacting with subunit B at a sub-region R_{B3} of the dimeric interface (Fig. 2a).

Based on the relative height of dimer peak to hexamer peak in the gel filtration chromatography results for WT hUGDH and its mutants, dimer-forming propensities were assigned. The dimer-forming propensity of WT hUGDH was set to 1, and those of hUGDH mutants were assigned from a maximum 5 to a minimum of 0 (Table 1).

Overall changes of modeled structures

Table 2 shows the overall conformational changes of WT hUGDH and its single mutants observed after homology modeling and energy minimization against the crystal structure. The overall conformational changes were measured by root-mean-square deviation (RMSD). The structures of homology-modeled mutants were practically identical to the WT crystal structure. Also, the energy-minimized structures showed little significant differences in overall structure. When the correlation coefficient (r) values between the RMSDs and the dimer-forming propensities were calculated, no significant correlations were observed for both the homology-modeled and the energy-minimized structures.

Predicted dynamics of WT hUGDH and its single mutants by NMA

The mean-square fluctuation (MSF) plots of each residue were calculated using eigenvalues and eigenvectors obtained from NMA for all the energy-minimized structures of WT hUGDH and its single mutants (Fig. 4a). The data show that the substitution of residues in the hUGDH structure triggers changes in the motional fluctuation patterns of the protein. The magnitude of motional fluctuation at various regions was measured from the MSF results and then correlations between the predicted motional fluctuations and the dimer-forming propensities were evaluated (Table 3). The motional fluctuations averaged over all residues showed a correlation of 0.53. Interestingly, the pattern of motional fluctuations at R_B, which consists of R_{B1} to R_{B4}, showed the strongest correlation ($r = 0.88$) among the four oligomeric interface regions. The sub-regions R_{B3} and R_{B4}, in particular, yielded dominant contributions to the correlation. R_C showed the second strongest correlation ($r = 0.57$) among the four oligomeric interface regions. The sub-regions R_{C1} and R_{C2} contributed critically to the correlation. On the contrary, R_E and R_F did not show meaningful correlations. When the correlation for all the oligomeric interface regions ($R_{B+C+E+F}$) was evaluated, the value notably increased to 0.95 (Fig. 5). No significant correlation ($r = 0.37$) was observed in regions that were not directly associated with the inter-subunit interactions (*not* $R_{B+C+E+F}$). $R_{\text{Active site}}$, which was defined as a region containing residues within 4 Å of any atom of NADH and UDP-glucose, showed a correlation of 0.63. Surface residues not belonging to the oligomeric interfaces ($R_{\text{Surface, not B+C+E+F}}$) showed a negative correlation ($r = -0.75$). Our results strongly demonstrate that the point mutations alter the dynamics profile of the enzyme computed from NMA. A large-magnitude cooperative motion at the oligomeric interfaces is a critical factor in interfering with the hexamer formation of the enzyme. R_B, in particular, dominantly contributes to this phenomenon, implying that motional stability at the dimeric interface is necessary to retain a hexameric quaternary structure of hUGDH.

Contribution of low-frequency modes to the correlations

We estimated the contribution of low-frequency normal modes to the correlations between motional fluctuation and dimer-forming propensity. The correlation coefficient values was plotted as a function of the number of the lowest frequency modes used for the calculation of the motional fluctuation at $R_{B+C+E+F}$ (Fig. 6). The correlation coefficient values vary highly up to 18 lowest modes

Table 3
Correlations between the magnitude of motional fluctuations at various regions and the dimer-forming propensity for WT hUGDH and its single mutants. $\langle \Delta x_R^2 \rangle$ is a motional fluctuation (Å^2) at a region, predicted by NMA.

Regions	$\langle \Delta x_R^2 \rangle$
R_B	0.88
R_{B1}	−0.41
R_{B2}	−0.11
R_{B3}	0.62
R_{B4}	0.73
R_C	0.57
R_{C1}	0.59
R_{C2}	0.70
R_{C3}	0.07
R_{C4}	−0.09
R_E	−0.26
R_{E1}	−0.08
R_{E2}	−0.13
R_{E3}	−0.50
R_F	0.06
R_{C+E+F}	0.16
$R_{B+C+E+F}$	0.95
not $R_{B+C+E+F}$	0.37
$R_{\text{Active site}}$	0.63
$R_{\text{Surface, not B+C+E+F}}$	−0.75
All residues	0.53

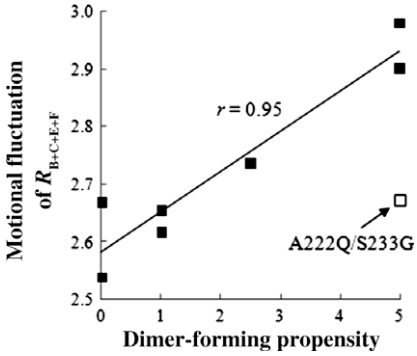

Fig. 5. Correlation between dimer-forming propensity and calculated motional fluctuation at $R_{B+C+E+F}$ for WT hUGDH and its single mutants. The motional fluctuation for a double mutant A222A/S233G is also displayed in the graph.

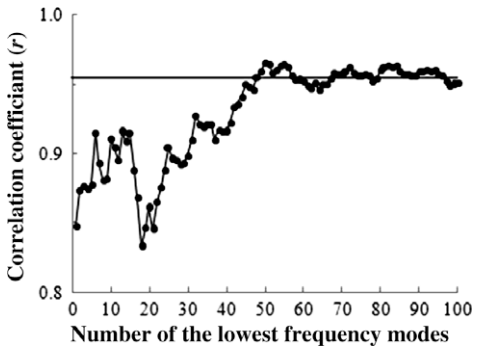

Fig. 6. Correlation between dimer-forming propensity and motional fluctuation at $R_{B+C+E+F}$ as a function of the number of the lowest frequency modes used to calculate the atomic mean-square fluctuation.

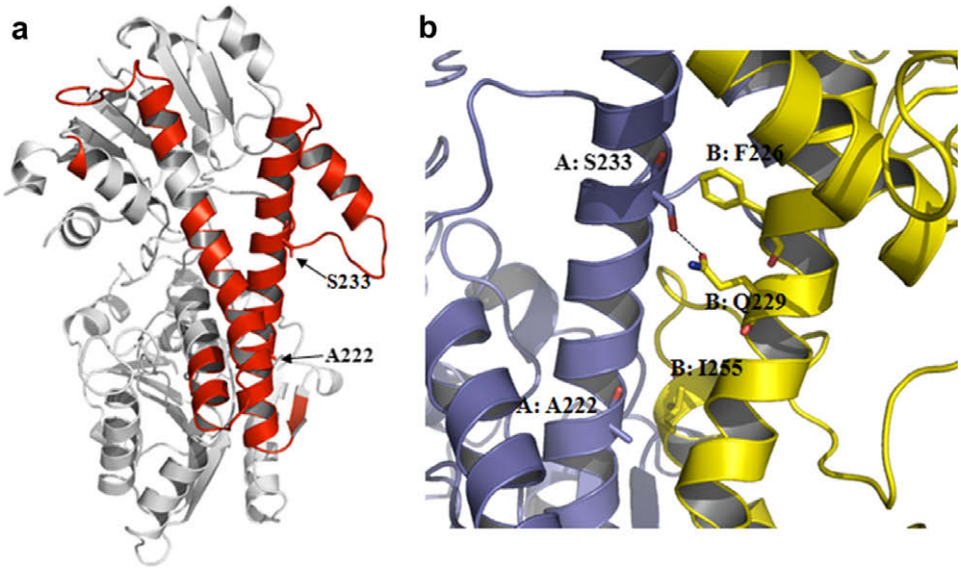

Fig. 7. Inter-subunit interactions by residues A222 and S233 in the double mutant A222Q/S233G. (a) Sub-regions showing relatively high correlations between the motional fluctuation calculated and the dimer-forming propensity ($r > 0.5$; R_{B3}, R_{B4}, R_{C1} and R_{C2}) are colored red. The residues A222 and S233 are shown as sticks. (b) A magnified image of the region at which the residues A222 and S233 are located. The hydrogen bond between A233 of subunit A and Q229 of subunit B is illustrated by a dotted line. (For interpretation of the references to colour in this figure legend, the reader is referred to the web version of this article.)

and then gradually increase up to 50 lowest modes. After the 50 lowest modes, the correlation coefficient values remain almost invariable. This means that the motional fluctuation is dominated by low-frequency modes and converges quickly as a function of the number of modes. It clearly demonstrates that the main contribution to the correlations was from the large-amplitude molecular motions along low-frequency modes.

Predicted dynamics of double mutant A222Q/S233G by NMA

NMA experiments for double mutant A222Q/S233G were performed. The calculated motional fluctuation was 2.67 for $R_{B+C+E+F}$, indicating the predicted value largely deviates from the expected correlation for WT hUGDH and all its single mutants (Fig. 5). Huh and colleagues reported that the double mutant A222Q/S233G was a dimer. They suggested that Ala222 and Ser233 might play important roles in maintenance of the hUGDH hexameric quaternary structure [27]. As seen in Fig. 7, Ala222 and Ser233 are located at the dimeric interface and form direct inter-subunit interactions. Ala222 makes a hydrophobic connection with Ile255. Ser233 forms a hydrogen bond with Gln229 and is in close contact with Phe226. Therefore, disruption of these interactions would likely change the dynamics of an oligomeric hUGDH, resulting in an increase of the motional fluctuation at the dimeric interface, R_B, which most prominently affects the hexamer formation of hUGDH. We suggest that the synergy between the intrinsic thermal fluctuation at the oligomeric interfaces and the increased dynamics at the dimeric interface determines the final oligomeric state of this double mutant A222Q/S233G hUGDH. Due to a large region leading to dimer formation, the local structural instability at the dimeric interface may not completely disrupt the dimer structure of hUGDH, which maintains the inter-subunit contacts in part. However, overall stable association at the dimeric interface seems to be of particular importance to sustain the hexameric quaternary structure.

Molecular basis for changes in motional fluctuation patterns

Our results show that the motional fluctuation at the oligomeric interfaces is associated with point-mutated residues that are considerably distant from the protein surface. Thus, how these "actions-at-a-distance" are generated is of major interest for understanding the correlation between the point mutations and the oligomer-forming propensity of WT hUGDH and its mutants.

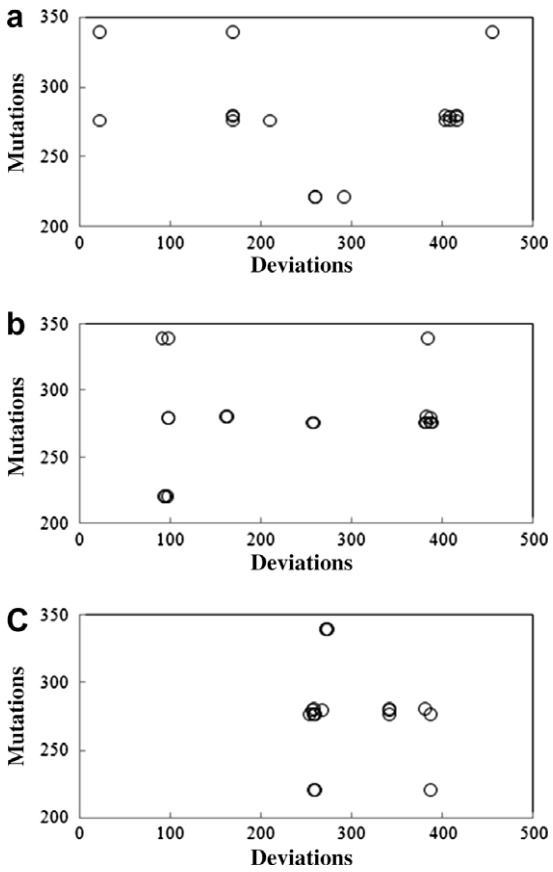

Fig. 8. Plots showing the correlation between the positions of mutations and the positions of the three largest deviations in the mutants. The deviations indicate the distance differences between Cα atom pairs of WT and mutants for (a) homology-modeled and (b) energy-minimized structures. The deviations in (c) are the MSF differences between the corresponding atom pairs of WT and mutants. The three positions of the largest deviations were selected within residue numbers 5–461.

In the MSF plots of Fig. 4a, black thick bars on the *x*-axis denote the oligomeric interface regions. Intriguingly, considerable regions of relatively large fluctuation are located at the oligomeric interfaces. For WT hUGDH, the average MSF values for $R_{B+C+E+F}$ and *not* $R_{B+C+E+F}$ were 2.65 Å^2 and 1.91 Å^2, respectively. The display of MSF in the hUGDH structure reveals that the flexible regions correspond to residues at the ends of the secondary elements and in the loops (Fig. 4b).

To correlate the highly affected regions to the point mutations, the positions of the mutations (*y*-axis) and the positions of the three largest deviations between WT and mutants (*x*-axis) were plotted (Fig. 8). The three largest distance differences between Cα atom pairs of WT and mutants for the homology-modeled and the energy-minimized structures were selected in Fig. 8a and b, respectively. The Fig. 8c shows the positions of the three largest MSF differences between the corresponding atom pairs of WT and mutants. For the homology-modeled structures, the sites of the largest deviation are dispersed in the structure (Fig. 8a). The sites of the largest deviation in the energy-minimized structures are relatively little dispersed and clustered at more flexible regions (Fig. 8b). When the graph was plotted by MSF deviations, the sites of the largest deviation were concentrated at all three positions (Fig. 8c). These three positions correspond to the large flexible regions 5, 7 and 8 of Fig. 4. These results strongly indicate that regardless of the site of mutation and its type, the perturbation triggered by the mutation is observed as large changes in protein dynamics at the specific regions remote from the mutated site (also see Fig. 4a). In the case of hUGDH, the effects originating at mutated sites tend to concentrate preferentially in the large flexible regions of the structure. Sinha and Nussinov analyzed proteins with the largest number of mutants in the PDB [28]. Their data showed that some regions are inherently more prone to adapt to the perturbations by the mutations. While the mutations were distributed over the entire sequence, the highest affected sites were at specific regions, especially the ends of the secondary elements and the loops. Our observation is consistent with the results obtained by Sinha and Nussinov.

Fig. 9a is an overlapped MSF plot for two representative hUGDH mutants that show distinct oligomeric states in solution (K220A and K279A have hexamer and dimer states, respectively). The regions in the K279A mutant that fluctuate significantly more than those in the K220A mutant are also displayed in the hUGDH structure (Fig. 9b). The figure shows that the residues of a large increased deviation are mainly located at the flexible regions of the oligomeric interfaces. These indicate that an increase in magnitude of the motional fluctuation at the oligomeric interfaces in K79A is mainly attributed to that at the flexible regions of the interfaces, resulting in interference with the hexamer formation of the enzyme.

It is a key issue to elucidate the mechanism of the "action-at-a-distance" or "allostery" of dynamic proteins. However, despite this increasing attention, how energetic strain initiating at the mutation site transmit through the residue network is still an open and debated question [29]. Many experimental studies have shown that point mutations can trigger protein motions at locations extending beyond the directly affected site. Leatherbarrow and Matthews carried out experiments with chymotrypsin inhibitor 2. They showed changes in the dynamics of a tryptophan side chain in response to an R to A mutation 13 Å away [30]. Clarkson and Lee introduced two mutations, V14A and V54A, into the serine protease inhibitor Eglin *c* and measured ^{15}N and ^{2}H NMR spin relaxation properties of these mutants. They observed that the effects of single amino acid substitutions clearly extend far beyond the point of mutation in both cases [31]. Biophysical evidences like these indicate that single mutation can cause far-reaching dynamics effects.

The results by Sinha and Nussinov revealed that structural perturbations caused by residue substitutions at diverse locations tend to be reflected preferentially at specific sites, regardless of their spatial distance from the substituted site and the types of the substituted residues [28]. They also mentioned that this observation implies that the residue substitution causes the changes in the energy landscape, resulting in a redistribution of the substrates in the ensemble of conformations populated under native conditions. Our results show that perturbations triggered by point mutations are observed as large changes in protein dynamics preferentially at the specific regions remote from the mutated site.

Conclusions

Our results show that single point mutations alter the dynamics of the enzyme around an energy minimum. The perturbation caused by residue substitution at sites far from the oligomeric interfaces is reflected preferentially as changes in intrinsic dynam-

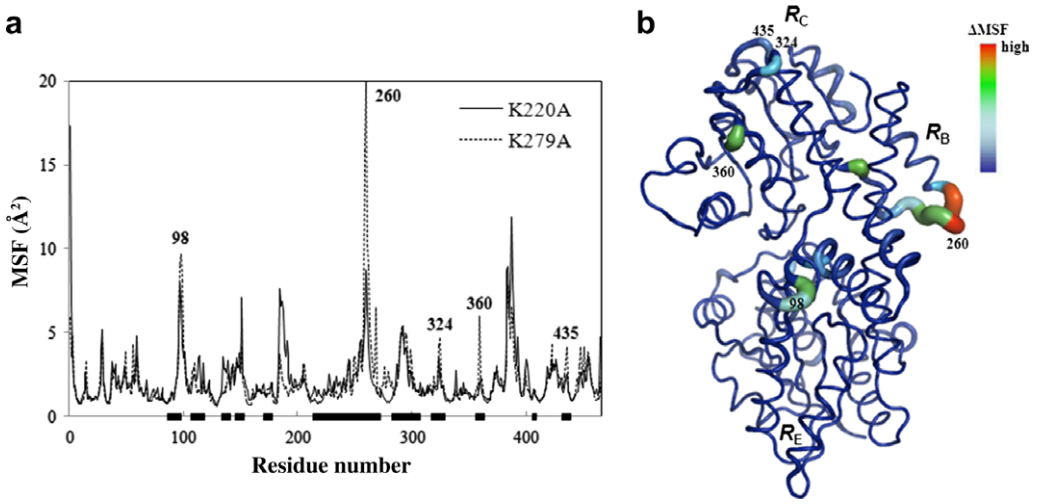

Fig. 9. NMA results for two representative hUGDH mutants of K220A and K279A. (a) MSF plots for the two mutants. Black thick bars on the horizontal axis of the plot denote the oligomeric interface regions. We also display the approximate positions of regions in K279A where the fluctuation significantly increased compared to that in K220A. (b) The regions showing a significantly increased fluctuation are displayed in the hUGDH structure by tube. The tube color and diameter represent the magnitude of the deviation.

ics at specific sites, especially the large flexible regions in the hUGDH structure. It affects the motional fluctuation pattern at oligomeric interfaces. We found that the magnitude of the motional fluctuations at the oligomeric interfaces, which results from the large-amplitude molecular motions along low-frequency modes, significantly correlates with the quaternary-structure-forming propensity of WT hUGDH and its mutants. A large-magnitude cooperative motion at the oligomeric interfaces interferes with the hexamer formation of the enzyme. Overall structural stability at the dimeric interface, in particular, appears to be necessary to retain the hexameric quaternary structure of hUGDH. We established the importance of the intrinsic thermal motion in the protein oligomerization problem. Considering the lack of structural data on the oligomeric states of WT hUGDH and its mutants, such a computational approach to characterize the dynamics of the protein would help rationalize the relationship between the structures and functions of the enzyme.

Acknowledgments

This work was supported by the Korea Research Foundation (KRF-2006-C00508) and Asan Institute for Life Sciences (2008-307). We thank Dr. Yoon for allowing us to use his MacroModel.

References

[1] J.S. Franzen, J. Ashcom, P. Marchetti, J.J. Cardamone Jr., D.S. Feingold, Biochim. Biophys. Acta 614 (1980) 242–255.
[2] R.H. Tukey, C.P. Strassburg, Annu. Rev. Pharmacol. Toxicol. 40 (2000) 581–616.
[3] P.L. Jansen, G.J. Mulder, B. Burchell, K.W. Bock, Hepatology 15 (1992) 532–544.
[4] D. Vigetti, M. Ori, M. Viola, A. Genasetti, E. Karousou, M. Rizzi, F. Pallotti, I. Nardi, V.C. Hascall, G. De Luca, A. Passi, J. Biol. Chem. 281 (2006) 8254–8263.
[5] R.V. Iozzo, J.D. San, Antonio, J. Clin. Invest. 108 (2001) 349–355.
[6] E.M. Selva, N. Perrimon, Adv. Cancer Res. 83 (2001) 67–80.
[7] P. Auvinen, R. Tammi, J. Parkkinen, M. Tammi, U. Agren, R. Johansson, P. Hirvikoski, M. Eskelinen, V.M. Kosma, Am. J. Pathol. 156 (2000) 529–536.
[8] B.P. Toole, T.N. Wight, M.I. Tammi, J. Biol. Chem. 277 (2002) 4593–4596.
[9] S. Cumberledge, F. Reichsman, Trends Genet. 13 (1997) 421–423.
[10] K. Ropponen, M. Tammi, J. Parkkinen, M. Eskelinen, R. Tammi, P. Lipponen, U. Agren, E. Alhava, V.M. Kosma, Cancer Res. 58 (1998) 342–347.
[11] M.A. Simpson, C.M. Wilson, J.B. McCarthy, Am. J. Pathol. 161 (2002) 849–857.
[12] R.E. Campbell, S.C. Mosimann, I. Van De Rijn, M.E. Tanner, N.C. Strynadka, Biochemistry 39 (2000) 7012–7023.
[13] K.E. Easley, B.J. Sommer, G. Boanca, J.J. Barycki, M.A. Simpson, Biochemistry 46 (2007) 369–378.
[14] http://www.rcsb.org/pdb.
[15] H.J. Berendsen, S. Hayward, Curr. Opin. Struct. Biol. 10 (2000) 165–169.
[16] K.A. Henzler-Wildman, M. Lei, V. Thai, S.J. Kerns, M. Karplus, D. Kern, Nature 450 (2007) 913–916.
[17] J. Ma, Structure 13 (2005) 373–380.
[18] A. May, M. Zacharias, Proteins 70 (2008) 794–809.
[19] S.E. Dobbins, V.I. Lesk, M.J. Sternberg, Proc, Natl. Acad. Sci. USA 105 (2008) 10390–10395.
[20] N. Floquet, S. Dedieu, L. Martiny, M. Dauchez, D. Perahia, Arch. Biochem. Biophys. 478 (2008) 103–109.
[21] B.J. Sommer, J.J. Barycki, M.A. Simpson, J. Biol. Chem. 279 (2004) 23590–23596.
[22] A. Sali, T.L. Blundell, J. Mol. Biol. 234 (1993) 779–815.
[23] R.B. Lehoucq, D.C. Sorensen, C. Yang, ARPACK user's guide, Rice University, Houston, 1997.
[24] I. Kolossváry, G.M. Keserü, J. Comput. Chem. 22 (2001) 21–30.
[25] I. Kolossváry, W.C. Guida, J. Comp. Chem. 20 (1999) 1671–1684.
[26] S. Hayward, A. Kitao, N. Go, Protein Sci. 3 (1994) 936–943.
[27] J.W. Huh, S.J. Yang, E.Y. Hwang, M.M. Choi, H.J. Lee, E.A. Kim, S.Y. Choi, J. Choi, H.N. Hong, S.W. Cho, J. Biochem. Mol. Biol. 40 (2007) 690–696.
[28] N. Sinha, R. Nussinov, Proc, Natl. Acad. Sci. USA 98 (2001) 3139–3144.
[29] C.J. Tsai, A. Del, Sol, R. Nussinov, Mol. Biosyst. 5 (2009) 207–216.
[30] R.J. Leatherbarrow, S.J. Matthews, Magn. Reson. Chem. 30 (1992) 1255–1260.
[31] M.W. Clarkson, A.L. Lee, Biochemistry 43 (2004) 12448–12458.